Langmuir

ARTICLE

pubs.acs.org/Langmuir

Self-Assembled Monolayers of Disulfide Cu Porphyrins on Au Surfaces: Adsorption Induced Reduction and Demetalation

M. Verónica Rivas,[†] Lucila P. Méndez De Leo,[†] Mariana Hamer,[‡] Romina Carballo,[‡] and Federico J. Williams[†,*]

[†]Departamento de Química Inorgánica, Analítica y Química Física, INQUIMAE-CONICET, Facultad de Ciencias Exactas y Naturales, Universidad de Buenos Aires, Buenos Aires, Argentina

[‡]Departamento de Química Analítica y Fisicoquímica, Facultad de Farmacia y Bioquímica, Universidad de Buenos Aires, Buenos Aires, Argentina.

ABSTRACT: Metalloporphyrin molecules have a wide range of potential applications in diverse technological areas ranging from electronics to optoelectronics, electrochemistry, photophysics, chemical sensors, and catalysis. In particular, self-assembled monolayers of porphyrin molecules have recently attracted considerable interest. In this work we have studied for the first time the self-assembly of a novel Cu deutero porphyrin functionalized with disulfide moieties using electrochemical techniques, UV−vis absorption spectroscopy, polarization modulation infrared reflection absorption spectroscopy, and photoelectron spectroscopies (XPS and UPS). Experimental results indicate that the molecule adsorbs retaining its molecular integrity without forming molecular aggregates via the formation of Au−S covalent bonds. Furthermore, the monolayer consists of a packed array of molecules adsorbed with the plane of the porphyrin molecule at an angle of around 30° with respect to the surface normal. Interestingly, adsorption induces reduction of the Cu center and its consequent removal from the center of the porphyrin ring resulting in porphyrin demetalation. Our results are important in the design of self-assembled monolayers of metallo porphyrins where not only blocking of the metal center by the functional groups that drive the self-assembly should be considered but also possible adsorption induced demetalation with the consequent loss in the properties imparted by the metal center.

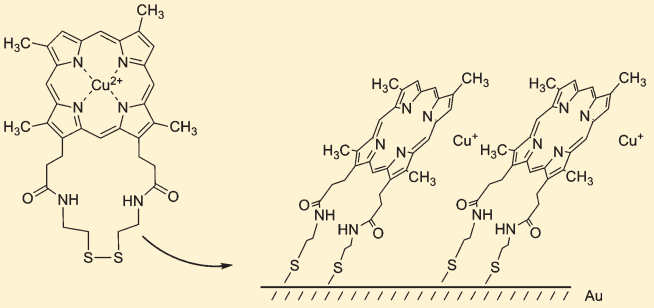

INTRODUCTION

Organic surfaces play a major role in material science thus a great diversity of methods have been employed to prepare organic thin films on solid surfaces. Functionalized self-assembled monolayers (SAMs) have attracted much attention because of their potential application in chemical sensors, biosensors, molecular switches, molecular electronics, etc.[1−3] SAMs provide a convenient, flexible, and simple way to tailor the interfacial properties of metals, metal oxides, and semiconductors. SAMs are organic assemblies which organize spontaneously and are formed by the adsorption of molecular constituents from solution or the gas phase onto solid surfaces. The molecules that form SAMs have a chemical functionality with a specific affinity for the substrate. In particular organothiols are well suited for fabricating structurally well-defined adlayers of monolayer thickness on gold, silver, palladium, and platinum[3] surfaces. It is well-known that organosulfur compounds react with gold surfaces[4] forming S−Au covalent bonds resulting in monolayer molecular assemblies. These ultrathin monolayers expose an organic surface with properties that can be tailored by varying the type of organothiol employed.

Porphyrins are a ubiquitous class of naturally occurring molecules involved in a wide variety of important biological processes. The common feature of all of these molecules is the basic structure of the porphine macrocycle, which consists of a 16-atom ring containing four nitrogen atoms, obtained by linking four tetrapyrrolic subunits with four methine bridges (see Figure 1 below). The size of the macrocycle is perfect to bind a great number of metal ions which can be inserted in its center forming metalloporphyrins. The diversity of their functions is in part due to the variety of metals that bind to the porphyrin ring. Porphyrin rings are found in a variety of important biological systems where they are the active site of numerous proteins, whose functions range from oxygen transfer and storage (hemoglobin and myoglobin) to electron transfer (cytochrome c and cytochrome oxidase) and energy conversion (chlorophyll).

The involvement of porphyrins in many biological processes and the possibility to tailor their physical and chemical properties at the molecular level, including very large dipole moments, polarizability, nonlinear optical response, energy transfer, and catalytic properties, make porphyrins and metalloporphyrins extremely versatile synthetic base materials. Therefore porphyrin-based films on metal or semiconductor surfaces[5] as well as org-

Received: June 3, 2011
Revised: July 28, 2011
Published: July 29, 2011

dx.doi.org/10.1021/la2020836 | *Langmuir* 2011, 27, 10714–10721

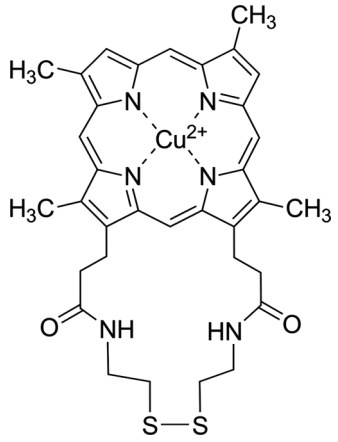

Figure 1. Cu deutero IX porphyrin disulfide (CuPorSS).

anized assemblies of porphyrins on metal surfaces have attracted recent considerable attention,[6−8] mainly because of the strong characteristic UV/vis absorption features of porphyrin chromophores[9,10] plus its potential application in light harvesting devices,[11] chemical sensors,[12] and photocatalysts[13] and as models for electron transfer reactions.[14] The key in the implementation of hierarchical assembly of porphyrins for the construction of molecular-based devices is the ability to readily create assemblies that can be reliably organized and attached to surfaces with a controlled molecular structure. The most widely employed method to bind porphyrin molecules to metal surfaces has been the formation of SAMs via the derivatization of porphyrins with thiol groups despite the fact that the thiol functional groups can coordinate the central metal ion of the porphyrin, resulting in multilayer formation as well as the blocking of the catalytic center.[10] Other strategies involve (i) preparation of SAMs containing imidazole-terminated adsorbates which bind covalently to a series of metalloporphyrins,[15] (ii) covalent attachment of metalloporphyrins to dimercaptoalkane modified gold electrodes,[16] (iii) formation of a pyridinethiol SAM followed by axial attachment of the metaloporphyrin,[17] and (iv) funtionalization of metalloporphyrins with disulfide groups.[18]

In the work presented here the Cu deutero IX porphyrin (CuPorSS) macrocycle bearing a disulfide moiety shown in Figure 1 was synthesized as a platform for the rapid, high yield attachment of these molecules to gold surfaces. Adsorption of CuPorSS over Au surfaces results in the formation of thiol tethered porphyrin self-assembled monolayers. This surface assembly was characterized utilizing X-ray and UV photoelectron spectroscopies (XPS and UPS), polarization modulation infrared reflection absorption spectroscopy (PMIRRAS), UV−visible absorption spectroscopy, and electrochemical measurements.

We found that CuPorSS forms a pack array of molecules that is bonded to the Au substrate via two covalent Au−S bonds, with the thiolated legs close to perpendicular to the surface and the porphyrin ring at an angle of around 30° with respect to the surface normal. Furthermore, adsorption results in reduction of the Cu metal ion followed by its consequent removal from the center of the porphyrin ring. As a result these monolayers are not stable in aqueous solutions as Cu ions leached away from the Au surface.

EXPERIMENTAL SECTION

Materials. Cu (II) deutero IX Porphyrin, cystamine.2HCl, *N*-acetylcysteamine, and (3-aminoporpyl)-trietoxysilan 99% (APTES) were obtained from Sigma-Aldrich. Tetrahydrofuran (THF), iso-butyl chloroformate, and triethanolamine were purchased from Merck. Ethylene chloride, methanol, and absolute ethanol were of analytical grade.

Porphyrin Disulfide Synthesis and Characterization. The Cu porphyrin with the disulfide moiety was prepared from Cu deutero porphyrin as described in the literature with minor modifications.[18] In short, the carboxylic acid functions of the Cu(II) deutero porphyrin were activated by treatment with iso-butyl chloroformate in THF in the presence of triethyl amine followed by addition of cystamine. In the same way, the metal free deutero IX porphyrin (PorSS) with the disulfide moiety has been synthesized. CuPorSS was characterized by matrix-assisted laser desorption/ionization time of flight (MALDI TOF) resulting in the expected molecular weight of 688 g/mol. Furthermore PorSS was characterized by ^{1}H NMR (300 MHz; $CDCl_3$) resulting in the following signals: δ (ppm) = 3.28 (2t, 2x$\mathbf{CH_2}CH_2CONHR$); 3.51; 3.59; 3.61; 3.63 (4s, 4x$\mathbf{CH_3}$); 4.25 (4t, NH$\mathbf{CH_2}\mathbf{CH_2}$S−S$\mathbf{CH_2}\mathbf{CH_2}$NH); 4.27 (2t, 2x$CH_2\mathbf{CH_2}$CONHR); 8.95 (2s, 2 H); 9.86; 9.90; 9.92; 10.11 (4s, 4 H meso). It should be noted that the NMR signals of the NH groups at the center of the porphyrin ring are lost due to the tautomerism observed in all porphyrins.

Preparation of Au Substrates. Silicon (100) substrates were coated with a 20 nm titanium and 20 nm palladium adhesion layer and a 200 nm gold layer, thermally evaporated with an Edwards Auto 306 vacuum coating system at $P < 10^{-8}$ bar. Au surfaces were cleaned electrochemically by cycling the electrode potential in 2 M sulfuric acid between 0 and 1.6 at 0.1 V s^{-1}. The electrochemically active areas were calculated from the reduction peak of gold. Semitransparent gold substrates used for UV−vis experiments were prepared according to Wanunu et al.[8] Briefly, glass substrates were first cleaned with piranha solutions for 20 min, then treated with 1:1:2 H_2O_2:NH_3:H_2O at 70 °C for 20 min, followed by copious rinsing with water and methanol. The substrates were then shaken in a 10% solution of APTES in methanol for 3 h, rinsed and sonicated in methanol, and dried under a N_2 stream. Glass substrates were coated with a 15 nm gold layer thermally evaporated and annealed (200 °C, 20 h). Prior to use the substrates were cleaned by UV/ozone (UVO Cleaner model 42, Jelight) for 15 min.

Monolayer Preparation. Self-assembled monolayers of CuPorSS were prepared in liquid phase by immersing the gold substrate into a freshly prepared 100 μM solution in methylene chloride for 24 h at room temperature in the absence of light. A final and careful rinsing was made with methylene chloride before drying under N_2. SAMs of *N*-acetylcysteamine were prepared in liquid phase by immersing the gold substrate into a freshly prepared 100 μM solution in absolute ethanol for 24 h at room temperature in the absence of light. A final and careful rinsing was made with ethanol before drying under N_2.

Photoelectron Spectrocoscopy. XPS and UPS measurements were performed under UHV conditions (base pressure $<5 \times 10^{-10}$ mbar) in a SPECS UHV spectrometer system equipped with a 150 mm mean radius hemispherical electron energy analyzer and a nine channeltron detector. XPS spectra were acquired at a constant pass energy of 20 eV using a Mg Kα (1253.6 eV) source operated at 12.5 kV and 20 mA and a detection angle of 30° with respect to the sample normal on grounded conducting substrates. Quoted binding energies are referred to the Au $4f_{7/2}$ emission at 84 eV. No charge compensation was necessary and no differential charging features were observed (e.g., low binding energy tails) given that we have measured sufficiently thin films on grounded conducting substrates. Atomic ratios were calculated from the integrated intensities of core levels after instrumental and photoionization cross section corrections. UPS spectra were acquired at a constant pass energy of 2 eV using a He I radiation source (21.2 eV) operated at 1.5 kV and 100 mA with normal detection. Samples were biased −8 V in order to resolve the secondary electron cutoff in the UPS spectra. Work function values were determined from the width of the UPS spectra as discussed below.

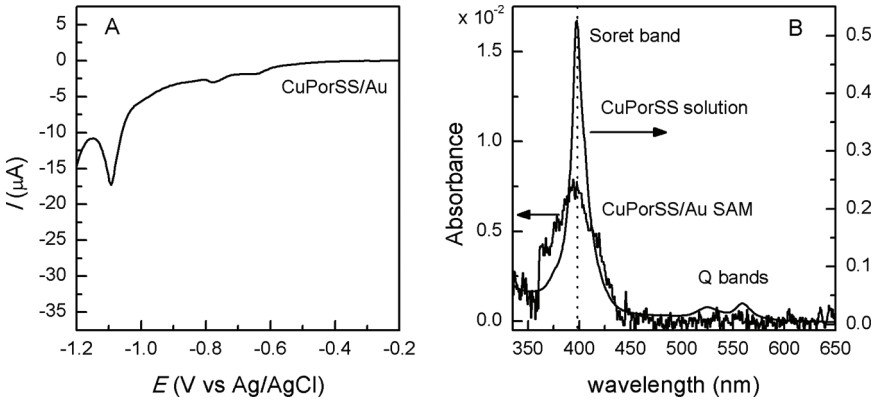

Figure 2. (a) Reductive desorption curve of CuPorSS monolayers on Au surfaces recorded at 0.05 V s^{-1} in 0.1 M NaOH. (b) UV−vis spectra of CuPorSS monolayers on Au surfaces (left axis) and in CH_2Cl_2 solution (right axis).

IR Spectroscopy. PMIRRAS experiments were performed on a Thermo Nicolet 8700 spectrometer equipped with a custom-made external tabletop optical mount, a MCT-A detector (Nicolet), a photoelastic modulator, PEM (PM-90 with II/Zs50 ZnSe 50 kHz optical head, Hinds Instrument), and syncronous sampling demodulator, SSD, (GWC Instruments). The IR spectra were acquired with the PEM set for a half wave retardation at 1500 cm^{-1}. The angle of incidence was set at 80°, which gives the maximum of mean square electric field strength for the air/gold interface. The signal was corrected by the PEM response using a method described by Frey et al.[19] Typically 1500 scans were performed and the resolution was set for 4 cm^{-1}. Transmission spectra for solid porphyrins were measured using KBr pellets. Resolution was set to 4 cm^{-1} and 200 scans were performed.

Electrochemical Measurements. Electrochemical measurements were carried out with an Autolab V 30 system (Eco Chemie). Gold substrates were mounted in a conventional three-electrode glass cell. Solutions were purged with argon. All potentials were measured and reported with respect to a Ag/AgCl (3 M KCl) reference electrode. Solutions were prepared using deionized H_2O from a Milli-Q purification system (Millipore Products, Bedford). Reductive electrodesorption of thiols from the Au substrates were performed by scanning the potential from −0.2 to −1.7 at 0.05 V s^{-1} in 0.1 M NaOH aqueous solution, at room temperature.

UV−Visible Spectroscopy Measurements. Transmission spectra were obtained with a Shimadzu UV-1603 UV−vis spectrophotometer. Spectra were recorded in the range 300−700 nm and are normalized with respect to the spectrum corresponding to the clean Au substrate used for monolayer formation.

RESULTS AND DISCUSSION

It is well-known that the reductive desorption of thiol-containing monolayers gives a voltammetric cathodic peak in aqueous solutions due to the cleavage of S−Au thiolate bonds.[20] We have therefore carried out electrochemical measurements in order to estimate the coverage and the electrochemical stability of CuPorSS self-assembled monolayers. In these measurements the charge density of the peak allows an estimation of the thiolate coverage. Figure 2A shows a typical curve corresponding to the reductive desorption of CuPorSS monolayers over Au surfaces. The observed curve shows a defined cathodic current peak preceding the hydrogen evolution reaction at a peak potential of E_p = −1.1 V vs Ag/AgCl. The position of the peak reflects that the SAM is desorbed from the Au substrate by reducing the S−Au bond. It is well-known that peak position depends both on the strength of the S−Au bond and on the lateral interactions in the monolayer and it could be in the range −0.8 to −1.2 V.[20] Assuming one electron per thiolate bond for the reductive desorption (2 per molecule), the charge density involved in the CuPorSS desorption peak of 6 samples yields an average surface coverage of $1.9 \pm 0.8 \times 10^{14}$ molecules cm^{-2}. This value is larger than that expected from the molecular area corresponding to molecules adsorbed with the porphyrin ring parallel to the Au surface (0.3×10^{14} molecules cm^{-2}).[21] Therefore the coverage calculated from the desorption curves implies that either the CuPorSS SAMs form monolayers oriented in a geometry with the porphyrin ring not parallel to the substrate or that CuPorSS binds parallel to the substrate forming molecular aggregates.

Figure 2B shows the UV−visible absorption spectra of CuPorSS in solution (right axis) and of a self-assembled monolayer of CuPorSS deposited over semitransparent Au substrates (left axis). The spectrum observed in solution is the typical spectrum of a metalloporphyrin consisting of two distinct regions. In the near-UV region we observe an intense absorption peak known as the Soret band (397.5 nm) and in the visible region we observe two small bands known as the Q bands (524.5 and 560 nm) which have much smaller extinction coefficients.[22] Given that the spectrum corresponding to a metal free-porphyrin has four Q bands, the observed spectrum with two Q bands confirms the presence of the Cu ion at the center of the porphyrin. The UV absorption spectrum of CuPorSS SAMs over Au surfaces shows a Soret band located at the same position (397.5 nm) as the band corresponding to the molecule in solution with no discernible shoulders. The implications of these observations are that (i) the molecule retains its optical properties after adsorption over the Au surface and (ii) no molecular J aggregates are formed in the monolayer as this would have resulted in a larger wavelength shift in the Soret band[9,23,24] (J -aggregates is a polymolecular state in which molecules are packed together in a plane-to-plane fashion). Furthermore from the calculated extinction coefficient and the UV absorption intensity of 6 samples we estimated a CuPorSS average surface coverage of $1.8 \pm 0.6 \times 10^{14}$ molecules cm^{-2}. This value is in complete agreement with the value estimated from the electrochemical measurements discussed above, and together with the fact that the molecules are not forming aggregates, it indicates that the porphyrin ring is not parallel to the Au surface. Here we should note that the UV−vis spectrum of CuPorSS SAMs over Au surfaces (Figure 2B left axis) shows no peaks in the Q-band region as they have very small extinction coefficients.

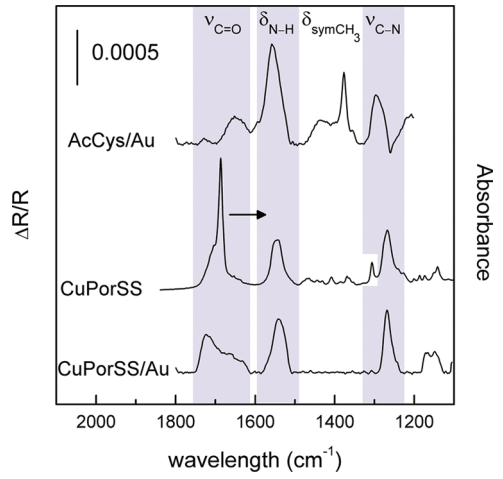

Figure 3. PMIRRAS spectra of self-assembled monolayers of CuPorSS and AcCys on Au surfaces (left axes). Resolution was set to 4 cm^{-1} and 1500 scans were performed. Transmission FTIR spectrum of CuPorSS in a KBr pellet (right axes). Resolution was set to 4 cm^{-1} and 200 scans were performed.

In order to characterize the adsorption geometry of surface CuPorSS porphyrins we carried out PMIRRAS measurements. Figure 3 shows a PMIRRAS spectrum of self-assembled CuPorSS molecules on Au surfaces. CuPorSS infrared transmission spectrum was also measured for comparison with the monolayer spectrum and shown in the right axes. Furthermore, self-assembled monolayers of *N*-acetylcysteamine (AcCys) on Au surfaces were also measured and shown in Figure 3. This compound has the same thiolated tail as the CuPorSS molecules, with a methyl group instead of the porphyrin group at the end of the tail and its spectrum will be important to rationalize the CuPorSS spectrum. Spectral assignments are shown in Table 1 below.

No significant signals from the porphyrin ring are observed in the monolayer spectrum and the most prominent peaks correspond to the amide group of the molecules resulting in three well-defined regions: amide I, II, and III.[25,26] The region at around 1700 cm^{-1} corresponds to C═O stretching absorption ($\nu_{C=O}$ amide I). The band at around 1540 cm^{-1} can be assigned principally to N−H deformation coupled to C−N−H bending (δ_{N-H} amide II), and the band at 1267 cm^{-1} corresponds to a C−N stretching mode coupled with CNH angle opening (ν_{C-N} amide III). In the KBr pellet, the amide I peak appears at 1686 cm^{-1}, the value expected for secondary amides.[25] A broadening and a shift to higher wavenumbers occurs when the CuPorSS molecules are adsorbed on the gold surface. Changes of the C═O frequencies toward higher wavenumbers of amides can occur because of bond strain. This phenomenon has been reported for lactams (cyclic monosubstituted amides).[25−27] In unstrained ring lactams (6 or more carbon atoms) the carbonyl absorption band appears at the same wavenumbers as in noncyclic amides, i.e., around 1640−1680 cm^{-1}, but shifts to higher frequencies in smaller rings. To look further into this matter, we measured a PMIRRAS spectrum of a gold substrate modified with N-acetylcysteamine as this compound has the same thiolated leg as the adsorbed porphyrin molecules. Therefore, we expect that the amide group in AcCys will not be strained due to geometric constraints when self-assembled on the surface. In fact, the AcCys PMIRRAS spectrum shows the position of the C═O stretching band at 1651 cm^{-1}, implying that, the shift of the C═O stretching band observed in the CuPorSS SAM can be attributed to constrains in the amide bond. Regarding the amide bond configuration, the wavenumbers where amide II and III bands appear correspond to secondary amides in a trans configuration.[25,26] The absence of bands at 1490−1440 and 1350−1310 cm^{-1} would correspond to secondary amides in a cis configuration implies that most of the amide groups are trans in these porphyrins. Another conclusion that can be drawn from the position of the amide I and II peaks in the IR spectra is that no significant hydrogen bonding between amide groups is present in the SAMs. The shifts observed for amide I and amide II peaks after self-assembling on gold occur in the opposite direction that H-bonding would have caused.[28]

Table 1. Spectral Mode Assignment of PMIRRAS Spectra of Self-Assembled Monolayers of AcCys (Left Column) and CuPorSS (Middle Column) on Au Surfaces as Well as Transmission FTIR of CuPorSS in a KBr Pellet (Right Column)

	AcCys (cm^{-1})	CuPorSS (cm^{-1})	
assigment	monolayer	monolayer	KBr pellet
$\nu_{C=O}$	1651	1722	1686
δ_{N-H}	1558	1542	1541
$\delta_{sym\ CH3}$	1377		1307
$\nu_{C=N}$	1296	1269	1267
		1173	1147

PMIRRAS spectra could be used to estimate the average molecular orientation as the integrated band intensities of absorbed molecules is proportional to $\cos^2\theta$, where θ is the angle between the average direction of the dipole moment and the surface normal.[29,30] Figure 3 shows a difference in relative intensity of the amide peaks between random distributed porphyrins (KBr pellet) and self-assembled porphyrins. This difference is due to the preferential orientation of surface adsorbed porphyrins. When the molecules are randomly oriented (in a KBr pellet), the amide I absorption is stronger than the amide II and amide III bands, indicating that the molecular extinction coefficient of amide I is larger. However, the PMIRRAS spectrum of the CuPorSS SAMs shows that the amide II and amide III absorption bands are stronger that the amide I absorption band. This fact suggests a close to parallel orientation of the C═O bond with respect to the surface (amide I intensity decreases) while the C−N bond lies close to perpendicular to the surface (amide II and III intensity increases). It is well-known that alkanethiols chains form a 20−30° angle with respect to the surface normal.[31,32] Therefore we expect that the thiolated alkyl legs of the porphyrin molecule would form a 20−30° angle with respect to the surface normal while the C═O would lie close to parallel to the surface and the porphyrin ring would form an angle of around 20−40° with respect to the surface normal. This adsorption geometry is in agreement with the fact that the porphyrin molecules do not form surface aggregates and with the estimated surface coverage. It is important to remark that C═O is not, on average, parallel to the surface because in that case no absorption peak for amide I would have been observed.

CuPorSS self-assembled monolayers on Au surfaces were further characterized with UPS and XPS. Figure 4A shows the UP spectra of CuPorSS monolayers on Au surfaces in comparison to the spectrum of the clean gold surface. The main graph shows the secondary electron cutoff and the inset shows the

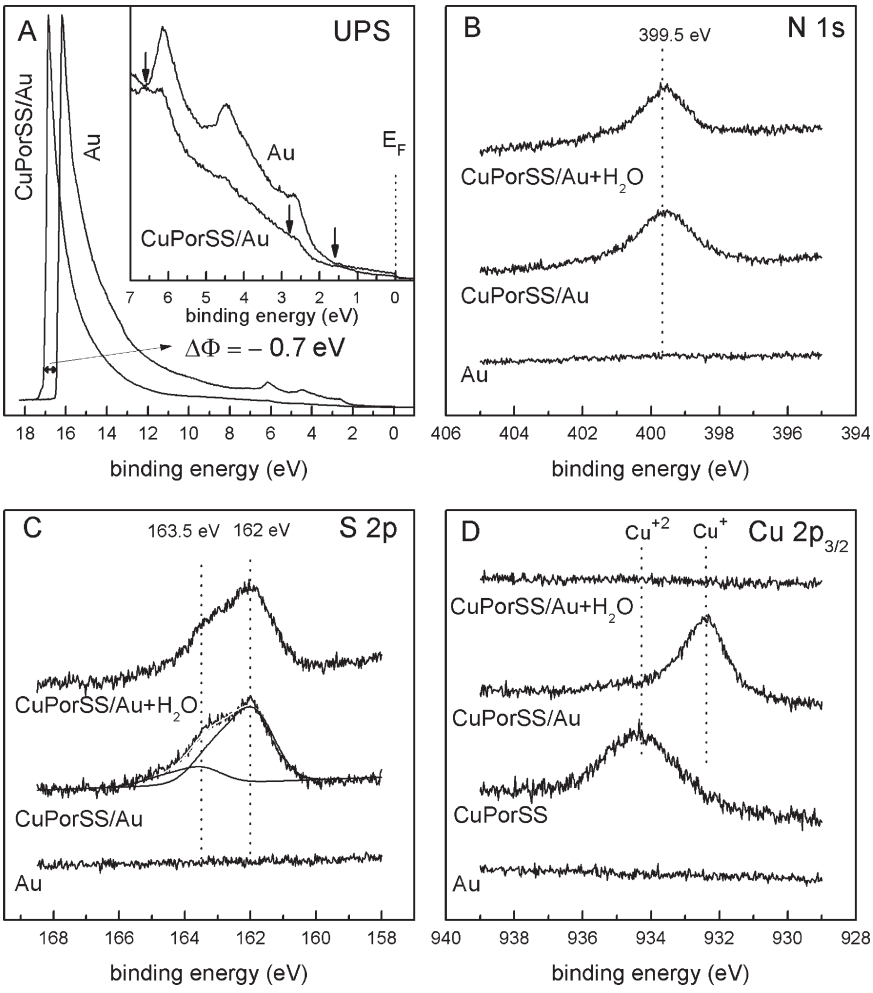

Figure 4. (A) UP spectra (He I) of a bare Au surface and CuPorSS on Au surfaces. The inset shows a magnified view of the region around the Fermi edge, whereas the mainframe shows the secondary electron cutoffs. (B) N 1s and (C) S 2p of CuPorSS monolayers on Au surfaces before and after immersion in water solution and of the bare Au surface. (D) Cu $2p_{3/2}$ XP spectra of (i) bare Au substrate, (ii) CuPorSS evaporated over Au, (iii) CuPorSS monolayers on Au surfaces, and (iv) CuPorSS/Au after immersion in H_2O solution.

region around the Fermi edge. The UPS spectrum corresponding to the bare Au substrate shows the same pattern and peak positions (2.7, 4.3, and 6.1 eV vs E_F) to that previously reported for clean Au surfaces and corresponds to the 5d bands.[33] From the width (W) of the UPS spectrum we can calculate the work function (Φ) of our Au substrates: $\Phi = 21.2$ eV $- W = 4.8$ eV which is in excellent agreement with values reported for polycrystalline gold.[31] When CuPorSS is adsorbed on the metal surface, the Au 5d bands decrease in intensity indicating the presence of the adsorbate.[34] The three highest occupied molecular orbitals of Cu porphyrin molecules are located at approximately 1.6, 2.8, and 6.6 eV vs E_F ($\Phi = 4.8$ eV),[35] these values are indicated with arrows in the CuPorSS UPS spectrum shown in the inset of Figure 4A. Clearly, the expected UPS signals corresponding to CuPorSS monolayers are not discernible as they have very little intensity (1.6 eV) or they are hidden by the Au 5d bands (2.8, 6.6 eV). The discernible feature in the monolayer spectrum is the shift in the position of the secondary electron cutoff which indicates a change in the work function of $\Delta\Phi = -0.7$ eV after formation of the CuPorSS SAM. We should bear in mind that the work function change caused by thiol SAMs over gold surfaces can vary over a wide range (-2 to $+2$ eV) depending on the functional group at the end of the organic molecule.[36] The CuPorSS induced work function modification is in complete agreement with values previously reported for methyl terminated SAMs on Au surfaces giving also an indication that the molecules adsorb with the porphyrin plane close to perpendicular to the surface plane and the methyl groups pointing away from the surface.[37,38]

Survey XPS scans show the presence of C, O, N, S, Au, and Cu with no other elements being observed on the CuPorSS/Au SAM. Figure 4 shows the XP spectra of the (b) N 1s, (c) S 2p, and (d) Cu $2p_{3/2}$ regions corresponding to a CuPorSS SAM on Au before and after after immersion of the Au covered substrate in a H_2O solution (see the discussion below). Signals corresponding to the bare Au substrate are shown for comparison. In the Cu $2p_{3/2}$ region, we also show the spectra corresponding to a CuPorSS thick film (evaporated over a Au substrate). The N 1s spectrum of CuPorSS SAMs over Au surfaces (Figure 4B) shows only one peak centered at 399.5 eV indicating that the 2 N atoms in the amide bonds are not greatly shifted with respect to the 4 N atoms in the porphyrin ring in agreement with other metalloporphyrin SAMs.[30] Most importantly the XPS determined N:Cu ratio is 6:1 in excellent agreement with the stoichiometry of the

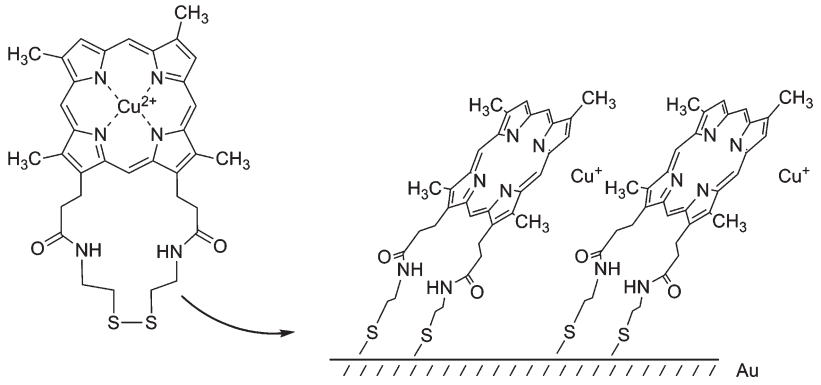

Figure 5. Scheme showing the proposed reduction of the metal ion and its consequent removal from the center of the porphyrin plane upon formation of the self-assembled monolayer.

molecule and demonstrates that the integrity of the porphyrin thiol molecules is retained after SAM formation. Furthermore from the integrated N 1s XPS intensity and the Cu $2p_{3/2}$ XPS intensity (see the discussion below) corresponding to the Cu-PorSS SAM over Au, we can estimate a surface coverage of $1.7 \pm 0.6 \times 10^{14}$ molecules cm^{-2}, value obtained after measuring six different samples. This value is in excellent agreement with the coverage estimated from the electrochemical reductive desorption as well as the UV−vis absorption measurements discussed above.

The S 2p XP spectrum of the CuPorSS SAM (Figure 4C) shows a broad signal with a high binding energy shoulder that can be accordingly fitted with two sets of doublets each corresponding to the S $2p_{3/2}$ and S $2p_{1/2}$ components with an spin orbit coupling of 1.2 eV.[34] The low binding energy contribution is centered at 162 eV and corresponds to thiol chemisorbed onto the gold substrate (bound thiol),[34] whereas the high binding energy contribution is centered at 163.5 eV and can be attributed to the presence of disulfide bonds which are not covalently bonded to the gold substrate (unbound thiols).[34] This later signal accounts for 15% of the total S 2p signal and could be due to a very small amount of porphyrin molecules that are incorporated into the SAM by lateral interactions with neighboring CuPorSS molecules with the disulfide bond pointing away from the surface.

The Cu $2p_{3/2}$ binding energy position reflects the oxidation state of the Cu ion in the metallo porphyrin. It is well established that Cu^+ has a Cu $2p_{3/2}$ peak at 932.3 eV whereas the peak corresponding to Cu^{2+} is shifted more than 1.2 eV toward higher binding energy and is therefore located at BEs > 933.7 eV.[39] Figure 4D shows the Cu $2p_{3/2}$ spectra corresponding to (i) CuPorSS thick films evaporated over Au surfaces, (ii) CuPorSS SAM over Au surfaces, and (iii) CuPorSS SAM after immersion in a water solution. The spectrum corresponding to the CuPorSS thick films shows a peak at 934.3 eV corresponding to the presence of Cu^{2+} atoms at the center of the porphyrin ring. This is the expected oxidation state for Cu metalloporphyrins given that Cu^{2+} is a d^9 ion with a preference for a square planar geometry and little tendency to add axial ligands.[40] On the other hand, the d^{10} Cu^+ metal ion prefers a tetrahedral geometry,[41] a state the rigid porphyrin ligand can never adapt. Furthermore, the relative good fit of the Cu^{2+} ion into the porphyrin center also explains the lack of any Cu^+ porphyrin complexes. Moreover, it has been reported that reduction of Cu^{2+} in acidic solutions (pH <4) leads to protonation and demetalation due to the larger radius of Cu^+.[40]

When Cu^{2+} deutero porphyrins with disulfide functionalities adsorb on Au surfaces forming a self-assembled monolayer, we observed a 2 eV shift in the position of the Cu $2p_{3/2}$ XPS peak to lower binding energies resulting in a peak position of 932.3 eV. This gives a clear indication that the oxidation state of Cu in the self-assembled monolayer is reduced probably to the Cu^+ oxidation state. Here we should point out that the observed reduction of the Cu^{2+} ion is not an experimental artifact due to the X-ray radiation, because the effect is only observed in the SAMs (is not observed in multilayer films) and because reduction of the metal ion in Cu^{2+} porphyrins under UHV conditions and irradiation with 1253.6 eV photons requires the presence of reducing species like Na.[42] The XPS observed reduction of the porphyrin Cu^{2+} ion to Cu^+ indicates charge transfer from the Au substrate to the metal ion suggesting a strong interaction between the porphyrin metal ion and the metal substrate. Reduction of metallo porphyrins and phthalocyanines (Pc) due to charge transfer from metal or semiconductor surfaces has been previously reported. Co tetraphenylporphyrin (TPP) multilayers have a Co $2p_{3/2}$ XPS peak at the typical Co^{2+} position (780 eV) that shifts 1.8 eV to lower BE in CoTPP monolayers on Ag(111). This finding has been ascribed to transfer of electron density from the Ag substrate to the Co ion, in conjunction with the formation of a covalent bond between metal center and substrate.[43] The same finding was reported for the adsorption of Co(II) octaethylporphyrin on Ag(111) where a 1.9 eV shift to lower BE is observed with respect to the multilayer film upon adsorption of the monolayer.[44] Similar observations have been made for Fe^{2+} TPP[45] and Fe^{2+} Pc on Ag(111);[46] where the lower BE shift in the Fe 2p XPS spectra is again attributed to charge transfer from the metal substrate to the metal ion. Finally, adsorption of CuPc on Si(111)[47] and on Al(100)[48] results in reduction of the Cu^{2+} metal ion to Cu^+. In line with previous work, we observe reduction of the porphyrin Cu metal ion after adsorption of CuPoSS molecules on Au surfaces. Also in line with previous work, we propose that charge transfer takes place via the overlap of a metal ion 3d orbital and electronic states of matching energy and symmetry of the Au surface forming new mixed states that take electrons from the Fermi sea. The implication is that electrons from the Au surface are transferred to the Cu ions causing their reduction.

As discussed above Cu^+ porphyrins are not known given the larger ionic radius of the Cu^+ metal ion and its preference to form complexes with a tetrahedral geometry. Therefore we propose that adsorption of the Cu^{2+} porphyrin from solution onto the Au surface causes not only reduction of the metal ion to Cu^+ but also its removal from the hole of the porphyrin ring (see Figure 5).

It is well-known that Cu^+ catalyzes the insertion of metal ions into porhyrin molecules by sitting on top of the porphyrin plane, deforming its core and thus favoring metal insertion from the opposite face of the porhyrin.[37] Consequently we propose that the Cu^+ metal ion is sitting on top of the porphyrin plane in the self-assembled monolayer. This would imply that the Cu ion in the SAM could easily escape the Cu porphyrin monolayer if it were to come in contact with aqueous solutions. We have therefore measured the N 1s, S 2p, and Cu $2p_{3/2}$ XPS spectra of CuPorSS SAM on Au surfaces after they have been immersed in water as well as in CH_2Cl_2 solutions (Figure 4B−D, top curves). Measurements show that the N 1s and S 2p XPS signals remain unmodified, while the Cu $2p_{3/2}$ signal disappears completely when the SAM is immersed in aqueous solutions whereas all signals remain unmodified in the second case. Therefore, immersion of CuPorSS SAM into aqueous solutions results in demetalation of the Cu ion, while the porphyrin molecules remain adsorbed on the Au surface. Further support for our interpretation of the XPS data is given by the fact that Cu^{2+} porphyrin molecules are not demetalated in CH_2Cl_2 solutions with added water (UV−vis spectra shows 2 Q-bands indicating the presence of the metal ion in the hole of the porphyrin).

CONCLUSIONS

We have shown that Cu(II) deutero porphyrin molecules with disulfide moieties can be successfully synthesized and used in the construction of self-assembled monolayers over Au surfaces. Porphyrin molecules adsorb by cleavage of the disulfide bond and formation of two S−Au bonds per adsorbed molecule as confirmed by electrochemical as well as XPS measurements. Furthermore, the integrity of the porphyrin macrocycle upon adsorption is determined by UV−vis absorption spectra that also help to rule out molecular aggregation in the monolayer. PMIRRAS measurements indicate that the molecules are adsorbed with the porphyrin plane tilted 20−40° with respect to the surface normal. This adsorption geometry is in excellent agreement with the surface coverage of 1.8×10^{14} molecules cm^{-2} estimated by three independent experimental techniques which indicate that porphyrin molecules form a pack array in the monolayer. Therefore the disulfide functional group serves not only as an excellent binding group that provides two S−Au covalent bonds but also it helps to direct the porphyrin ring in a direction close to perpendicular to the surface which could be very important in applications where this orientation would be useful. Most importantly, adsorption induces reduction of the Cu^{2+} metal ion to Cu^+ due to charge transfer from the metal substrate to the metal ion in complete agreement with previous work. We propose that this is followed by its consequent removal from the center of the porphyrin ring. This phenomenon results in demetalation of the porphyrin ring when the SAM is immersed in aqueous solutions. Our results are of prime importance in the design of molecular architectures based on self-assembled monolayers of metalloporphyrins, where not only the possible metal blocking by thiol functionalities should be considered but also possible adsorption induced demetalation with the subsequent loss in the properties imparted by the metal ion.

AUTHOR INFORMATION

Corresponding Author

*E-mail: fwilliams@qi.fcen.uba.ar.

ACKNOWLEDGMENT

Funding from CONICET, UBA, and Agencia is gratefully acknowledged. L.P.M.D.L., R.C., and F.J.W. are CONICET Fellows. R.C. and M.H. thank Prof. I. N. Rezzano for fruitful discussions.

REFERENCES

(1) Kriegisch, V.; Lambert, C. *Top. Curr. Chem.* **2005**, *258*, 257.
(2) Kind, M.; Wöll, C. *Prog. Surf. Sci.* **2009**, *84*, 230.
(3) Love, J. C.; Estroff, L. A.; Kriebel, J. K.; Nuzzo, R. G.; Whitesides, G. M. *Chem. Rev.* **2005**, *105*, 1103.
(4) Nuzzo, R. G.; Allara, D. L. *J. Am. Chem. Soc.* **1983**, *105*, 4481.
(5) Smith, A. R. G.; Ruggles, J. L.; Yu, A.; Gentle, I. R. *Langmuir* **2009**, *25*, 9873.
(6) Yang, J.; Li, M.; Li, H.; Yang, Y.; Kashimura, Y.; Wang, C.; Torimitsu, K.; Lu, X.; Hu, W. *J. Phys. Chem. C* **2010**, *114*, 12320.
(7) Mezour, M. A.; Cornut, R.; Hussien, E. M.; Morin, M.; Mauzeroll, J. *Langmuir* **2010**, *26*, 13000.
(8) Wanunu, M.; Vaskevich, A.; Rubinstein, I. *J. Am. Chem. Soc.* **2004**, *126*, 5569.
(9) Boeckl, M. S.; Bramblett, A. L.; Hauch, K. D.; Sasaki, T.; Ratner, B. D.; Rogers, J. W. *Langmuir* **2000**, *16*, 5644.
(10) Imahori, H.; Norieda, H.; Nishimura, Y.; Yamazaki, I.; Higuchi, K.; Kato, N.; Motohiro, T.; Yamada, H.; Tamaki, K.; Arimura, M.; Sakata, Y. *J. Phys. Chem. B* **2000**, *104*, 1253.
(11) Ochiai, T.; Nagata, M.; Shimoyama, K.; Amano, M.; Kondo, M.; Dewa, T.; Hashimoto, H.; Nango, M. *Langmuir* **2010**, *26*, 14419.
(12) Davis, J. J. *Chem. Commun.* **2005**, 3509.
(13) Schaming, D.; Allain, C.; Farha, R.; Goldmann, M.; Lobstein, S.; Giraudeau, A.; Hasenknopf, B.; Ruhlmann, L. *Langmuir* **2009**, *26*, 5101.
(14) Wang, Q.; Zhi, F.; Wang, W.; Xia, X.; Liu, X.; Meng, F.; Song, Y.; Yang, C.; Lu, X. *J. Phys. Chem. C* **2009**, *113*, 9359.
(15) Carvalho de Medeiros, M. A.; Cosnier, S.; Deronzier, A.; Moutet, J.-C. *Inorg. Chem.* **1996**, *35*, 2659.
(16) Pilloud, D. L.; Chen, X.; Dutton, P. L.; Moser, C. C. *J. Phys. Chem. B* **2000**, *104*, 2868.
(17) Zhang, Z.; Hou, S.; Zhu, Z.; Liu, Z. *Langmuir* **1999**, *16*, 537.
(18) Cordas, C. M.; Viana, A. S.; Leupold, S.; Montforts, F. P.; Abrantes, L. M. *Electrochem. Commun.* **2003**, *5*, 36.
(19) *Polarization-modulation Approaches to Reflection-Absorption Spectroscopy*; Frey, B. L., Corn, R. M., Weibel, S. C., Eds.; John Wiley & Sons: New York, 2001; Vol. 2, p 1042.
(20) Azzaroni, O.; Vela, M. E.; Martin, H.; Hernández Creus, A.; Andreasen, G.; Salvarezza, R. C. *Langmuir* **2001**, *17*, 6647.
(21) Shimazu, K.; Takechi, M.; Fujii, H.; Suzuki, M.; Saiki, H.; Yoshimura, T.; Uosaki, K. *Thin Solid Films* **1996**, *273*, 250.
(22) Wang, M. Y. R.; Hoffman, B. M. *J. Am. Chem. Soc.* **1984**, *106*, 4235.
(23) Imahori, H.; Hasobe, T.; Yamada, H.; Nishimura, Y.; Yamazaki, I.; Fukuzumi, S. *Langmuir* **2001**, *17*, 4925.
(24) Khairutdinov, R. F.; Serpone, N. *J. Phys. Chem. B* **1999**, *103*, 761.
(25) Bellamy, L. J. *The Infra-red Spectra of Complex Molecules*, 1958 ed.; Methuen & Co Ltd.: London, 1954.
(26) Lin-Vein, D.; Colthup, N. B.; Fateley, W. G.; Grasselli, J. G. *The Handbook of InfraRed and Raman Characteristic Frequencies of Organic Molecules*; Academic Press, Inc.: San Diego, CA, 1991.
(27) Chen, C. Y. S.; Swenson, C. A. *J. Phys. Chem.* **1969**, *73*, 2999.
(28) Clegg, R. S.; Hutchison, J. E. *Langmuir* **1996**, *12*, 5239.
(29) Zamlynny, V.; Lipkowski, J. Quantitative SNIFTIRS and PM IRRAS of Organic Molecules at Electrode Surfaces. In *Advances in Electrochemical Science and Engineering*; Alkire, R. C., Kolb, D. M., Lipkowski, J., Ross, P. N., Eds.; Wiley: Weinheim, Germany, 2006; Vol. 9.
(30) Chan, Y.-H.; Schuckman, A. E.; Perez, L. M.; Vinodu, M.; Drain, C. M.; Batteas, J. D. *J. Phys. Chem. C* **2008**, *112*, 6110.

(31) Porter, M. D.; Bright, T. B.; Allara, D. L.; Chidsey, C. E. D. *J. Am. Chem. Soc.* **1987**, *109*, 3559–3568.
(32) Grumelli, D.; Méndez De Leo, L. P.; Bonazzola, C.; Zamlynny, V.; Calvo, E. J.; Salvarezza, R. C. *Langmuir* **2010**, *26*, 8226–8232.
(33) Scudiero, L.; Barlow, D. E.; Mazur, U.; Hipps, K. W. *J. Am. Chem. Soc.* **2001**, *123*, 4073.
(34) Duwez, A. S.; Pfister-Guillouzo, G.; Delhalle, J.; Riga, J. *J. Phys. Chem. B* **2000**, *104*, 9029.
(35) Khandelwal, S. C.; Roebber, J. L. *Chem. Phys. Lett.* **1975**, *34*, 355–359.
(36) Heimel, G.; Romaner, L.; Brédas, J.-L.; Zojer, E. *Phys. Rev. Lett.* **2006**, *96*, 196806.
(37) Heinz, B.; Morgner, H. *Surf. Sci.* **1997**, *372*, 100.
(38) Marmont, P.; Battaglini, N.; Lang, P.; Horowitz, G.; Hwang, J.; Kahn, A.; Amato, C.; Calas, P. *Org. Electron.* **2008**, *9*, 419.
(39) Biesinger, M. C.; Lau, L. W. M.; Gerson, A. R.; Smart, R. S. C. *Appl. Surf. Sci.* **2010**, *257*, 887.
(40) Sanders, K. M.; Bampos, N.; Clyde-Watson, Z.; Darling, S. L.; Hawley, J. C.; Kim, H. J.; Mak, C. C.; Weeb, S. J. Axial Coordination Chemistry of Metalloporphyrins. In *The Porphyrin Handbook*; Kadish, K. M., Smith, K. M., Guilard, R., Eds.; Academic Press: New York, 1999; Vol. 3.
(41) Cotton, F. A.; Wilkinson, G. *Advanced Inorganic Chemistry*, 4 ed.; Wiley: New York, 1980.
(42) Niwa, Y. *J. Chem. Phys.* **1975**, *62*, 737.
(43) Flechtner, K.; Kretschmann, A.; Steinrück, H. P.; Gottfried, J. M. *J. Am. Chem. Soc.* **2007**, *129*, 12110–12111.
(44) Bai, Y.; Buchner, F.; Kellner, I.; Schmid, M.; Vollnhals, F.; Steinrück, H. P.; Marbach, H.; Gottfried, J. M. *New J. Phys.* **2009**, *11*, 125004.
(45) Buchner, F.; Flechtner, K.; Bai, Y.; Zillner, E.; Kellner, I.; Steinruck, H. P.; Marbach, H.; Gottfried, J. M. *J. Phys. Chem. C* **2008**, *112*, 15458–15465.
(46) Bai, Y.; Buchner, F.; Wendahl, M. T.; Kellner, I.; Bayer, A.; Steinrück, H. P.; Marbach, H.; Gottfried, J. M. *J. Phys. Chem. C* **2008**, *112*, 6087–6092.
(47) Dufour, G.; Poncey, C.; Rochet, F.; Roulet, H.; Sacchi, M.; De Santis, M.; De Crescenzi, M. *Surf. Sci.* **1994**, *319*, 251.
(48) Ruocco, A.; Evangelista, F.; Gotter, R.; Attili, A.; Stefani, G. *J. Phys. Chem. C* **2008**, *112*, 2016–2025.